Applied Catalysis B: Environmental 86 (2009) 206–215

Contents lists available at ScienceDirect

Applied Catalysis B: Environmental

journal homepage: www.elsevier.com/locate/apcatb

Influence of reaction products of K-getter fuel additives on commercial vanadia-based SCR catalysts
Part II. Simultaneous addition of KCl, $Ca(OH)_2$, H_3PO_4 and H_2SO_4 in a hot flue gas at a SCR pilot-scale setup

Francesco Castellino [a], Anker Degn Jensen [a,*], Jan Erik Johnsson [a], Rasmus Fehrmann [b]

[a] Department of Chemical and Biochemical Engineering, Technical University of Denmark, Building 229, DK-2800 Kgs. Lyngby, Denmark
[b] Centre for Sustainable and Green Chemistry, Department of Chemistry, Technical University of Denmark, Building 207, DK-2800 Kgs. Lyngby, Denmark

ARTICLE INFO

Article history:
Received 15 July 2008
Received in revised form 30 October 2008
Accepted 2 November 2008
Available online 14 November 2008

Keywords:
SCR
Deactivation
Vanadia
KCl
Polyphosphoric acid
Biomass

ABSTRACT

A commercial V_2O_5–WO_3–TiO_2 corrugated-type SCR monolith has been exposed for 1000 h in a pilot-scale setup to a flue gas doped with KCl, $Ca(OH)_2$, H_3PO_4 and H_2SO_4 by spraying a water solution of the components into the hot flue gas. The mixture composition has been adjusted in order to have P/K and P/Ca ratios equal to 2 and 0.8, respectively. At these conditions, it is suggested that all the K released during biomass combustion gets captured in P–K–Ca particles and the Cl is released in the gas phase as HCl, thus limiting deposition and corrosion problems at the superheater exchangers during biomass combustion. Aerosol measurements carried out by using a SMPS and a low pressure cascade impactor have shown two distinct particle populations with volume-based mean diameters equal to 12 and 300 nm, respectively. The small particles have been associated to polyphosphoric acids formed by condensation of H_3PO_4, whereas the larger particles are due to P–K–Ca salts formed during evaporation of the water solution. No Cl has been found in the collected particles. During the initial 240 h of exposure, the catalyst element lost about 20% of its original activity. The deactivation then proceeded at slower rates, and after 1000 h the relative activity loss had increased to 25%. Different samples of the spent catalyst have been characterized after 453 h and at the end of the experiment by bulk chemical analysis, Hg-porosimetry and SEM-EDX. NH_3-chemisorption tests on the spent elements and activity tests on catalyst powders obtained by crushing the monolith have also been carried out. From the characterization, it was found that neither K nor Ca were able to penetrate the catalyst walls, but only accumulated on the outer surface. Poisoning by K has then been limited to the most outer catalyst surface and did not proceed at the fast rates known for KCl. This fact indicates that binding K in P–K–Ca compounds is an effective way to reduce the negative influence of alkali metals on the lifetime of the vanadia-based SCR catalysts. On the other hand, P-deposition was favoured by the formation of the polyphosphoric acids, and up to 1.8 wt% P was accumulated in the catalyst walls. Deactivation by polyphosphoric acids proceeded at about 0.2% day^{-1}. About 6–7% of the initial activity was lost due to the accumulation of these species. However, the measured relative activity reached a steady-state level during the last 240 h of exposure indicating that the P-concentration in the bulk reached a steady-state level due to the simultaneous hydrolysis of the polyphosphoric acids.

1. Introduction

As described in Part I of this work [1], changes in the fly ash composition during biomass combustion are seen as a potential solution to both deposition and corrosion problems encountered on the super-heaters at power plants. These problems are mainly due to the formation of KCl aerosols experienced during biomass combustion, which are formed during cooling of the flue gas. The above mentioned changes in the ash composition may involve the addition of P- and Ca-compounds in the boiler in order to create the reaction conditions at which (i) the K released by the biomass during combustion is captured in P–K–Ca compounds having higher melting temperatures than KCl; and (ii) the Cl is released in the gas phase as HCl thereby avoiding chlorine-induced corrosion.

* Corresponding author. Tel.: +45 45 25 28 41; fax: +45 45 88 22 58.
E-mail address: aj@kt.dtu.dk (A.D. Jensen).

0926-3373/$ – see front matter © 2008 Elsevier B.V. All rights reserved.
doi:10.1016/j.apcatb.2008.11.008

Initial tests on P–Ca additives have shown up to 74–98% reduction in the Cl content of the deposits when the molar ratios of P/(K + Na) and P/Ca in the resulting fuel mixture were in the ranges 1.9–3.2 and 0.8–0.9, respectively [2]. For instance, similar values may be obtained by cofiring straw with about 13% meat and bone meal (MBM) on an energy basis.

The addition of these P- and Ca-compounds during biomass combustion and the corresponding changes in both ash load and composition may also have a beneficial effect on the fast SCR catalyst deactivation normally experienced during biomass combustion [3,4]. Here K, which is known as one of the strongest poisons for the vanadia-based catalysts normally used in the SCR process [5–11], once deposited as submicron particles of KCl and K_2SO_4, is found to easily diffuse inside the catalyst wall and thereby deactivate the active sites. The transfer of K to the catalyst, as shown in Part I of this work, apart from being related to the submicron particles, is directly dependent on how strongly K is bound to the particle itself. In this sense, capturing K into P–K–Ca particles may decrease the amount of K that is released to the catalyst surface and deactivate it. These particles will in fact have higher melting temperatures and potentially a higher stability.

On the other hand, both Ca and P are known as deactivating compounds for the vanadia-based SCR catalysts [5,6,12–15]. Having a relatively weak poisoning strenght, Ca is normally considered as a physically deactivating specie since during combustion it forms very stable compounds constituting the fly ash, which tend to block the pore structure of the catalyst wall. Furthermore, sulfation of the deposited Ca is often referred to form a fouling layer on the outer catalyst surface. On the other hand, P may act both as chemical and physical deactivating species according to the compounds it may form during combustion [15]. When polyphosphoric acids (PO_x) are formed, physical deactivation by pore blocking and surface masking is enhanced by the liquid viscous nature of these compounds. Furthermore, chemical deactivation at high concentrations (i.e. >100 ppmv) may be very fast and involves blocking of the catalytic cycle via formation of non-active V(4+) species [15]. Increasing the concentration in the flue gas of P and Ca by the addition process, which as stated above may require an excess of both species compared to K, may then lead to undesired deactivating effects. These may counterbalance the possible positive effects obtained by binding K into P–K–Ca particles.

The aim of this study is to evaluate the potential effects of the P, Ca addition process on the SCR catalysts by exposing a commercial vanadia-based SCR monolith to a flue gas doped with K, Ca and P for 1000 h and following its activity as a function of exposure time. The exposed catalysts are further characterized by a range of techniques.

2. Experimental

A water solution of KCl, $Ca(OH)_2$, H_3PO_4 and H_2SO_4 has been injected in a hot flue gas ($T > 900$ °C) from a natural gas burner. The resulting flue gas was then passed over a commercial SCR monolith, and the activity was periodically measured.

Both the setups and experimental procedures employed in the tests reported in this paper are the same as those described in Part I of this work, and are here only briefly introduced. For further details, see Ref. [1].

2.1. Catalysts

Commercial corrugate-type monoliths obtained from Haldor Topsøe A/S were used in this study. The catalysts were based on V_2O_5 (up to 5 wt%) and tungsten oxide (WO_3, up to 9 wt%) dispersed on a fibre reinforced TiO_2 carrier. The monoliths had a size of 75 mm × 75 mm × 500 mm. The hydraulic diameter of the channels was 6.44 mm. The wall thickness was about 1 mm. Pieces have been cut from both the fresh and spent monoliths in order to study their local properties under well defined reaction conditions in a laboratory fixed bed reactor. In order to run activity tests on powder samples, they have been gently crushed in a mortar and the particle fraction in the range 105–125 μm has been collected by sieving. The top and bottom 5 cm of the element were cut off after 453 h of exposure (indicated as "First cut" in this work), and the rest of the element was recharged in the reactor and the exposure restarted. In the following, the cut samples will be referred to as "ADD1T" and "ADD1B", respectively. Two more samples were then cut off at the end of the test from the top and bottom 5 cm of the recharged element. They will be referred to as "ADD2T" and "ADD2B", respectively.

2.2. SCR pilot plant

The SCR pilot plant setup used for this investigation is the same as described in [15]. It mainly consists of a natural gas burner for the flue gas production, a lance for spraying the aqueous solution, a square duct hosting a full length monolith and a NH_3 supply system. NH_3 is injected both in the burner to produce the desired NO concentration at the reactor inlet, and in the flue gas duct leading to the reactor for the NO reduction. Channel blocking is avoided by a soot blowing system installed at the reactor inlet.

2.3. K–P–Ca–S addition

In order to simulate the addition process, the molar P:K and P:Ca ratios in the flue gas have been fixed to 2 and 0.8, respectively. The KCl concentration has been fixed to 10 mg/Nm^3. Accordingly, 13, 26 and 20 mg/Nm^3 of $Ca(OH)_2$, H_3PO_4 and H_2SO_4 have been added. The addition has been carried out by preparing a water solution of the above listed compounds with the following concentrations: KCl = 6.7×10^{-3} mol/l, $Ca(OH)_2$ = 1.7×10^{-2} mol/l, H_3PO_4 = 1.3×10^{-2} mol/l, H_2SO_4 = 1.0×10^{-2} mol/l. In particular, H_2SO_4 was added in order to completely dissolve the different salts. Since the total flue gas flow at the injection point was equal to 50 Nm^3/h, the solution feed has been fixed to 1 l/h. Only 40 Nm^3/h were then let through the catalyst element during the whole exposure.

2.4. Aerosol measurements

Aerosol measurements were performed by using both a Scanning Mobility Particle Sizer (SMPS, TSI Inc.), which included an Electrostatic Classifier (Model 3080) and a Condensation Particle Counter (Model 3775), and a 10-stage Berner-type low pressure cascade impactor (LPI) with an aerodynamic diameter range of 0.03–12.7 μm connected to a vacuum pump. Sampling for the SMPS was made at the SCR reactor inlet by an ejector sampler running with dry, particle-free air. In the case of the LPI, the flue gas was sampled directly at the reactor inlet without any dilution. Both the sampling line and the LPI were therefore heated at 90 °C in order to avoid any water condensation.

2.5. Activity measurements

The rate of the SCR reaction at typical industrial reaction conditions has been assumed to follow an Eley-Rideal mechanism of reaction with NH_3 adsorbed on the catalyst surface and NO

reacting from the gas phase. The following expression for the rate of reaction, r_{NO}, can then be derived:

$$-r_{NO}(\mathrm{mol/m^3 s}) = kc_{NO}\frac{K_{NH_3}c_{NH_3}}{1+K_{NH_3}c_{NH_3}} \quad (1.1)$$

where k [1 s^{-1}] is the rate constant, c_{NO} and c_{NH_3} [mol/m^3] are the concentrations of NO and NH_3, respectively, and K_{NH_3} [m^3/mol] is the adsorption constant for NH_3 on the catalyst surface. The fraction term on the right-hand side of Eq. (1.1) is the NH_3 coverage of the catalytic surface, θ_{NH_3}.

At the pilot plant, the activities of the catalysts were measured at 350 °C in the presence of about 500 ppmv NO, 600 ppmv NH_3, 10 vol.% O_2, 6 vol.% CO_2, and about 10 vol.% H_2O.

Since ammonia in our measurements is added in excess with respect to NO (i.e. $NH_3/NO \approx 1.2$), the NH_3 coverage, θ_{NH_3}, can be assumed equal to 1 and the reaction rate can be regarded as pseudo-first order with respect to NO and zero order with respect to NH_3. Therefore, directly from the fractional NO conversion, X, it is possible to calculate an observed catalyst activity constant, k', that includes both the influence of external and internal mass transfer:

$$k'(\mathrm{ml/g\,s}) = -\frac{F_{gas}}{m_{cat}}\ln(1-X) \quad (1.2)$$

where F_{gas} is the gas flow rate (ml/s), m_{cat} is the weight of catalyst (g). The degree of deactivation can then be calculated as the ratio k/k_0 between the rate constant of the catalyst during exposure, k, and the one measured for the fresh element, k_0, right before starting the poison addition.

In the laboratory, powdered samples have been tested for activity in a packed bed quartz micro-reactor with a diameter equal to 10 mm. Around 0.07 g of powder has been used during activity measurements. This has been mixed with sand of the same particle size in order to have a particle bed of about 10 mm, thus ensuring the applicability of the here assumed integral reactor model. In all tests, the total flow was equal to 2.8 Nlitre/min constituted by 500 ppmv NO, 600 ppmv NH_3, 5 vol.% O_2 and 1.4 vol.% H_2O in N_2. Activity measurements have been performed in the temperature range 250–400 °C. The catalyst activity has been calculated according to Eq. (1.2) and the deactivation as the ratio between the activity constant of the spent catalyst and the one measured for the fresh one.

During all activity measurements, the NO concentration in the flue gas has been measured with a conventional UV analyzer (Rosemount NGA 2000). Due to the presence of water in the gas composition during all activity measurements, no N_2O formation is expected [16].

2.6. Ammonia chemisorption

NH_3 chemisorption tests have been periodically carried out at the pilot scale setup during exposure to the additive mixture. The measurements have been made at 350 °C and 40 Nm^3/h. Around 600 ppmv NH_3 has been added to the flue gas to the SCR reactor for 30 min in order to saturate the catalyst surface. During this saturation period, only the NO produced by the natural gas combustion was present (i.e. ≈80 ppmv). After this time, the NH_3 was shut off and right after, around 500 ppmv NO was produced by adding a different stream of NH_3 to the burner. The amount of chemisorbed NH_3 can then be calculated by integration over time the amount of reduced NO, due to the equimolar reaction between the gaseous NO and the chemisorbed NH_3.

2.7. Catalyst characterization

Small pieces of the catalyst were cut from the ends of both fresh and exposed monoliths and characterized without further treatment with respect to bulk chemical composition, mercury porosimetry and physical appearance by a Scanning Electron Microscope (SEM).

The chemical composition was obtained by ICP-OES at the laboratory of DONG Energy A/S. Prior to the measurements, the samples were cut to 1.5 × 1.7 cm^2 and dried at 105 °C for 2 h before analysis.

The total pore volume and the pore size distribution of the different catalyst samples were made by mercury intrusion in a Micromeritics Autopore II 9220 porosimeter. SEM-EDX analysis was performed at the Danish Technological Institute using a Zeiss Ultra55 and an Oxford ISIS with a Pentafet X-ray detector. In particular, the EDX analysis was performed on three different areas of about 200 μm × 200 μm for each sample. The numbers reported in this work are the averages of the different measurements. The standard deviations of the measurements have been found <0.2, 0.2, 0.5, 0.6 and 0.2 wt% for V, K, P, Ca and S, respectively.

3. Results

3.1. Aerosol measurements at the pilot-scale setup

3.1.1. SMPS measurements

Fig. 1 shows the particle size distribution (PSD) measured by the SMPS. The number-based distribution (Fig. 1a) is characterized by a peak around 9 nm. Due to their small sizes, these particles are very mobile and are expected to have fast deposition rates on the catalyst surface. The volume-based distribution (Fig. 1b), which is proportional to the mass carried by the different particles, shows instead the presence of two distinct peaks. The first one has a mean diameter equal to 12 nm, whereas the second one has a peak around 300 nm. This second peak is clearly representing most of the volume/mass of the total PSD.

The dual-mode volume-based PSD measured by SMPS indicate the presence of mainly two classes of compounds:

1. The first one is constituted by small particles and high concentration numbers due to homogeneous nucleation of gaseous species. This class of particles accounts for about 6% of the total volume measured by the SMPS.
2. The second class is constituted by bigger particles with low total concentration numbers. Their formation is likely due to salt crystallization during water evaporation from the atomized solution droplets at the injection point. This class accounts for about 94% of the total volume measured by the SMPS.

Due to their different mobility and number concentrations, these two particle classes contribute differently to the species accumulation and penetration into the catalyst walls.

3.1.2. Low pressure cascade impactor test

The results of the tests made with the LPI are shown in Fig. 2 and reported in Table 1. Here a mass-based particle size distribution with a peak at around 200 nm can be seen. This value is lower than the one measured by the SMPS, and the difference is believed to be due to experimental uncertainties associated with the different sampling techniques and equipments. Particle deposition was found to happen at every single impactor stage as indicated by the non-zero particle concentration in the whole particle diameter range. The total mass concentration was about 10 mg/Nm^3. The EDX chemical analysis of the collected deposits showed no Cl in

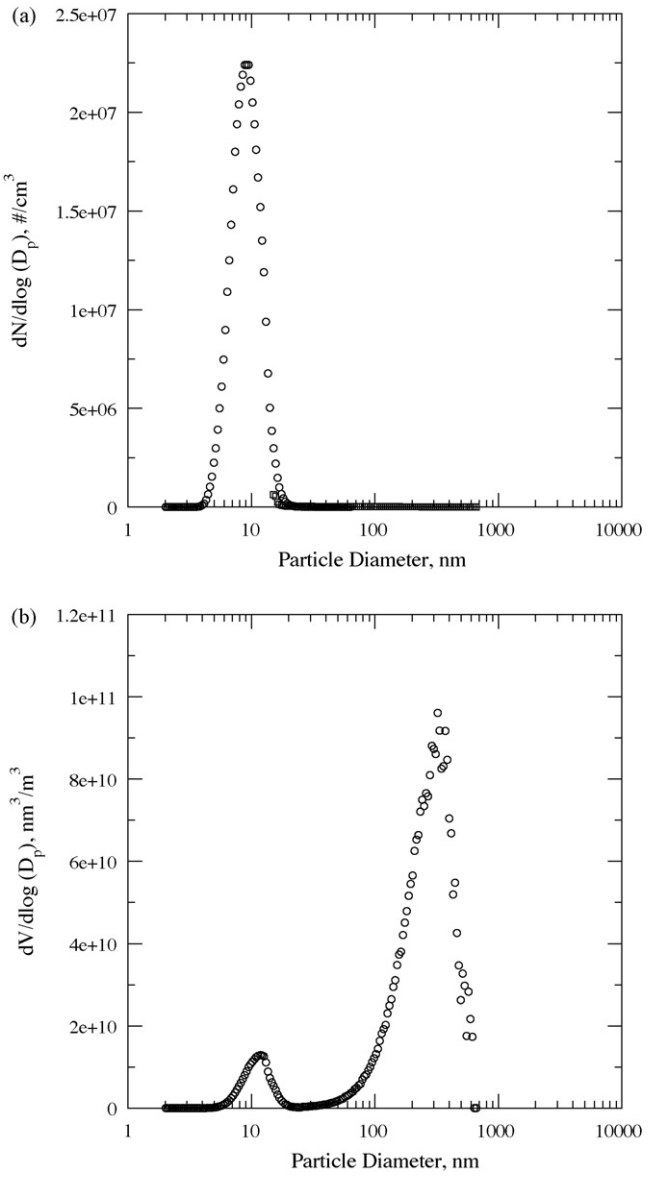

Fig. 1. Number-based (a) and volume-based (b) particle size distributions measured by a SMPS at the reactor inlet during simulatneous addition of KCl (10 mg/Nm^3), $Ca(OH)_2$ (13 mg/Nm^3), H_3PO_4 (26 mg/Nm^3) and H_2SO_4 (20 mg/Nm^3). T = 350 °C.

any of the impactor stages, indicating that Cl was effectively released to the gas phase prior to enter the SCR reactor. From the analysis of the element distribution shown in Fig. 2, it can be seen that both Ca and P are distributed in the particle diameter range

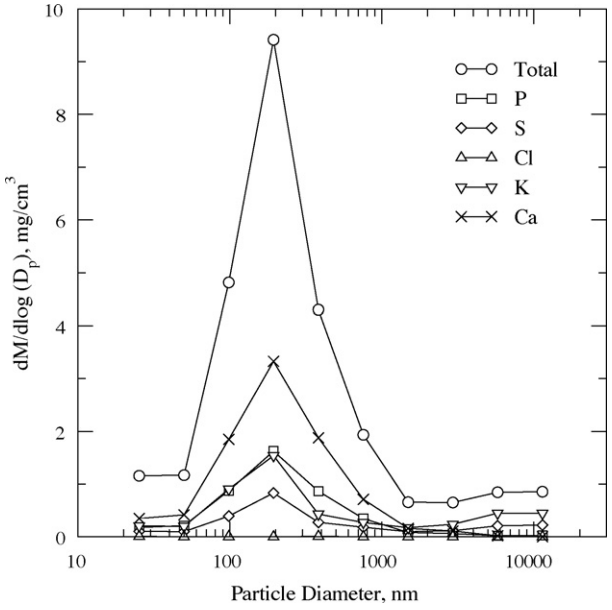

Fig. 2. Particle size distribution measured by a low pressure impactor at the reactor inlet during simulatneous addition of KCl (10 mg/Nm^3), $Ca(OH)_2$ (13 mg/Nm^3), H_3PO_4 (26 mg/Nm^3) and H_2SO_4 (20 mg/Nm^3). T = 90 °C. The curves for each single element have been obtained knowing their concentration on each single stage from EDX analysis.

25–3000 nm and are instead not found at higher diameters, where only K and S are found, probably due to the formation of some K_2SO_4. For each impactor stage, the different P:K, P:Ca, K:S and K:Ca molar ratios have been calculated and compared with the ones present in the injected solution. As it can be seen in Table 1, both P:Ca and K:S molar ratios have been found constant at around 0.65 and 1.55, respectively, throughout the whole particle size range, with only some exceptions for the P:Ca ratio at the first and second impactor stage. Simply based on these values it is not possible to identify the exact composition of the formed salts. However, by comparing the results with both the P:K and P:Ca injected, it is possible to conclude that some P is missing. This result might indicate the formation of gaseous P-compounds or the preferential formation of particles with diameters out of the impactor range, for instance those with volume-based mean diameter at 12 nm measured by the SMPS.

3.2. Catalyst characterization

3.2.1. Bulk and surface chemical analysis

Table 2 reports the results of both the bulk and surface analysis of samples taken from the exposed monolith at two different

Table 1
EDX analysis performed on the foils of the impactor stages.

Stage (#)	Particle diameter (nm)	P/K (mol/mol)	P/Ca (mol/mol)	K/S (mol/mol)	K/Ca (mol/mol)
1	11,391	0.08	17.22	1.63	211.61
2	5,773	0.06	1.42	1.76	23.63
3	2,931	0.33	0.72	1.67	2.18
4	1,488	0.62	0.68	1.44	1.10
5	754	1.60	0.63	1.23	0.39
6	382	2.53	0.60	1.28	0.24
7	194	1.33	0.63	1.52	0.47
8	98	1.22	0.61	1.88	0.50
9	50	1.35	0.66	1.63	0.49
10	25	1.08	0.66	1.64	0.61
Addition		2	0.8	0.67	0.4

Table 2
Bulk and surface chemical analysis for the fresh and spent monoliths.

	Fresh	ADD1T	ADD2T	ADD2B	ADD1B
Axial position (cm)		5	10	40	45
Additive exposure (h)		453	1000	1000	453
Bulk chemical analysis					
V% (wt/wt)	1.6	2.4	1.9	1.8	1.7
K% (wt/wt)	–	0.1	0.2	0.1	<0.1
P% (wt/wt)	–	0.7	1.8	1.3	0.5
Ca% (wt/wt)	1.7	2.1	1.9	1.7	1.8
S% (wt/wt)	0.3	0.4	0.4	0.3	0.3
Cl% (wt/wt)	<0.1	<0.1	<0.1	<0.1	<0.1
Surface chemical analysis					
V% (wt/wt)	2.10	3.84	3.35	1.93	2.04
K% (wt/wt)	–	0.22	0.25	0.33	0.12
P% (wt/wt)	–	1.67	4.67	3.10	1.72
Ca% (wt/wt)	–	0.41	0.36	1.17	0.11
S% (wt/wt)	0.66	0.67	0.71	1.39	0.36
Cl% (wt/wt)	–	–	–	–	–

exposure times. According to the results obtained from the bulk elemental analysis, P is, among the different species, the element that has accumulated the most in the catalyst walls: on average, the P-accumulation rate is equal to 1.4×10^{-3} wt%/h, corresponding to about 4% of the incoming P mass. Regarding the Ca and S, the elemental bulk analysis did not show any important increase of these two species in the exposed samples. In fact, apart from ADD1T, the contents of Ca and S were similar to the ones measured for the fresh catalyst, indicating very low accumulation rates for these two elements. The same can be said for the Cl, where the levels were below the lower detection limits for all tested samples.

The results of the EDX surface chemical analysis showed the presence of all the added elements but Cl on the outer surface of the catalyst wall. P was again the most abundant element with a concentration in the range 1.7–4.7 wt%. These values are higher than the total P found in the bulk. As it will be seen later, the reason for the difference is in the decreasing P-concentrations measured along the cross-section of the catalyst wall. As stated before, Ca and S are normally found in the bulk of the fresh catalyst, but are not seen on the outer surface of the walls by EDX. This fact indicates that their presence might be due to the glass fibres, which are reinforcing the catalyst support. All the exposed samples showed instead some Ca and S also on the outer surface indicating that some deposition of these elements did happen during the exposure to the additive mixture. K was also found on the outer surface. The highest level was found on ADD2B, where this was equal to 0.3 wt%, corresponding to a K:V molar ratio equal to 0.2. Comparing the P:K and P:Ca ratios on the catalyst surface with the ratios in the injected solution indicates an enhanced accumulation of P in the catalyst walls.

3.2.2. SEM analysis

Aerosol deposition on the outer catalyst surface has been confirmed by the SEM pictures taken of the different samples, shown in Fig. 3. In the case of ADD1T shown in Fig. 3a, most of the characteristic macro-cracks were filled with particles. However, these particles which were deposited in the catalyst macro-cracks were able to penetrate the pores for only 20–30 μm, as shown in Fig. 3b for ADD1B, indicating that clogging of the macro-cracks did not necessarily require the complete filling of their pore volume. Fig. 3c shows a picture at higher magnifications of the deposits found in the macro-cracks.

At the end of the exposure, the appearance of the catalyst surface had changed. The SEM analysis made after 1000 h of exposure revealed the presence of layer on the outer catalyst surface. Fig. 4 shows the surface of the catalyst at different

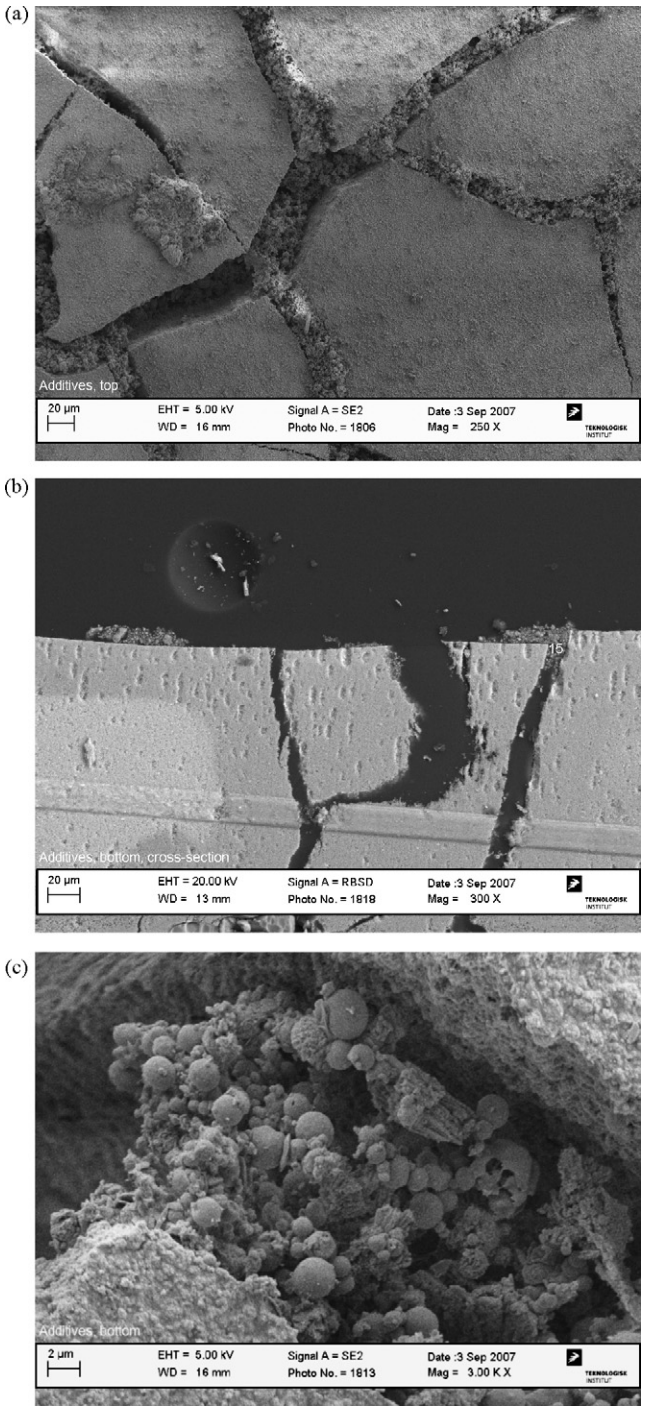

Fig. 3. SEM images of catalyst samples taken after 453 h of exposure: (a) ADD1T; (b) ADD1B; (c) ADD1B.

magnifications, together with pictures taken of a fresh sample at the same magnifications for comparison. This layer was revealed by the presence of unusual cracks on the surface as shown in Fig. 4a and b. As can be seen from these pictures, this layer appears as a compact phase about 2–3 μm thick. The comparison with the fresh sample surface clearly confirms the presence of this deposit covering the original catalyst surface. In fact, only the zones revealed by the deposit breakage somewhat recall the porous structure seen on the fresh sample. The EDX analysis of the zones underneath the formed layer, which were revealed by the outer layer cracks, had a reduced content of P compared to the top of the

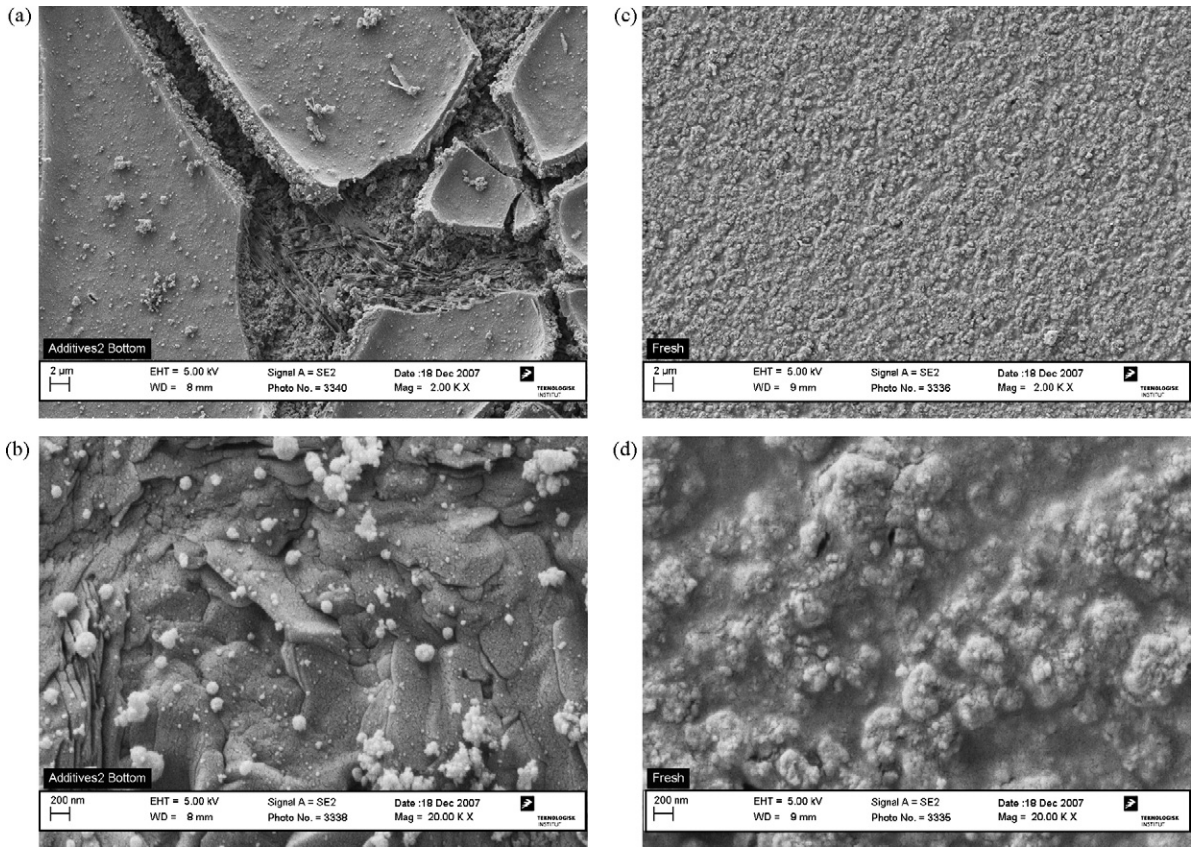

Fig. 4. SEM images of: (a and b) catalyst sample taken after 1000 h of exposure (ADD2B); (c and d) fresh sample. Magnification: (a and c) 2000×; (b and d) 20,000×.

compact layer itself: in the zones opened to the original catalysts material, the P-content was found equal to around 1 wt%, whereas the average P-content of the surface was equal to 3 wt%.

Cross-sections of the catalyst sample have also been analyzed by SEM-EDX in order to measure the distribution of the different elements inside the catalyst walls. The P-distribution for the sample ADD1B and ADD2T are shown in Fig. 5. The measured profiles were those typical for diffusion limited processes, with the P-concentrations levelling off within the first 100 μm of the catalyst wall. In the figure, it can also be seen how the P-levels have increased according to the longer exposure in the sample ADD2T.

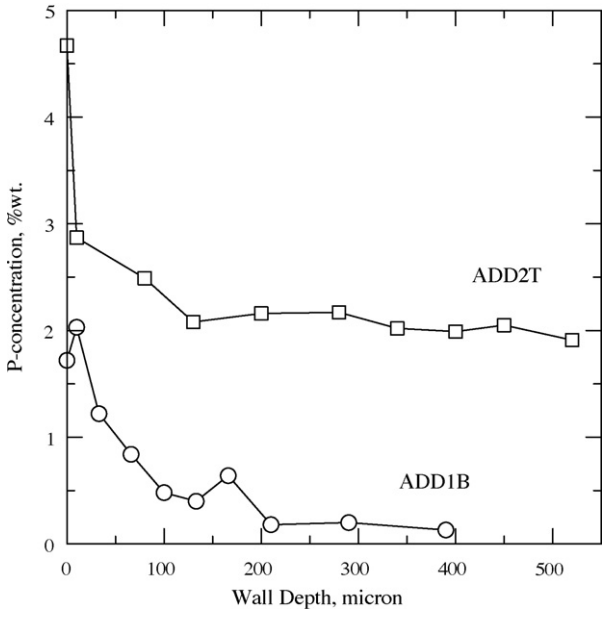

Fig. 5. P-concentration profile inside the spent catalyst walls.

Regarding K and Ca, they were not found inside the catalyst walls indicating the inability of these elements in diffusing into the catalyst material. Sulphur was constantly ranging inside the walls between 0.4 and 0.5 wt%, identical to the values found for a fresh sample.

Overall, the results obtained from the analysis of the catalyst cross-sections clearly indicate (i) the ability of P in penetrating the whole catalyst wall; (ii) the inability of K and Ca, although deposited on the outer surface, to further diffuse inside the wall.

3.3. Deactivation at the pilot-scale setup

3.3.1. Activity measurements

Three activity measurements made after 0, 191 and 1000 h of exposure, respectively, are shown in Fig. 6. As it can be seen, apart from the different final conversions obtained, which are also dependent on different total catalyst mass due to the cut after 453 h, the conversion curve obtained at 1000 h differs from the other two curves because it first goes through a maximum value right after the NH_3 introduction, and then reaches a steady-state value after about 2 min of exposure to NH_3. All the activity measurements made after around 300 h of exposure to the additive mixture have shown this behaviour. No NO conversion transient was instead measured at shorter exposure times, as shown by the activity tests made at 0 and 191 h of exposure. This NO transient was found in a previous investigation to be related to the accumulation of polyphosphoric acids in the catalyst wall and the subsequent titration of V(5+) active sites by formation of

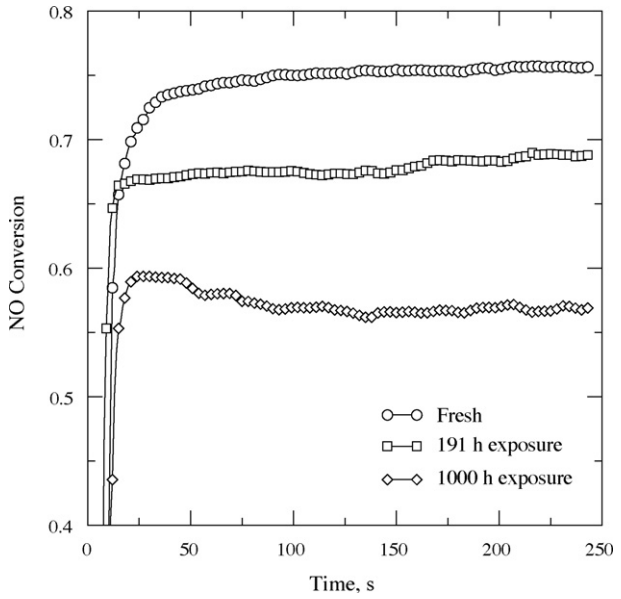

Fig. 6. Activity measurement made on fresh and spent monolith at 350 °C. Gas dry composition: NO = 500 ppmv, NH_3 = 600 ppmv, O_2 = 10 vol.%, CO_2 = 6 vol.%, H_2O = 10 vol.%. Flow: 40 Nm^3/h.

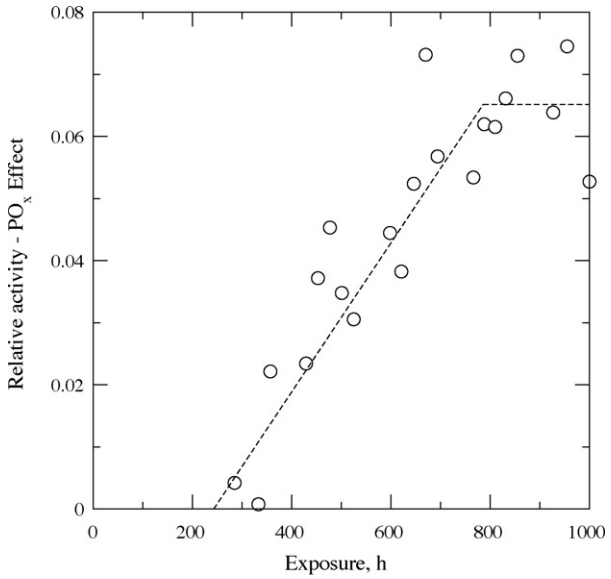

Fig. 8. PO_x deactivation effect as a function of exposure time. The data points represent the difference between "Max X" and "Steady-state X" curves in Fig. 6.

P–V(4+) species during exposure to NH_3 [15]. From both the aerosol measurements and the catalyst characterization presented so far, it is clear that also in this case the transient can be associated to the PO_x. In order to isolate the PO_x effect on the overall degree of deactivation, for each activity measurement both a maximum and a steady-state relative activity have been calculated. The results of the calculation are shown in Fig. 7. As it can be seen, the two curves separate from each other after about 300 h of exposure. Fig. 8 shows a plot of the difference between the "Max X" and the "Steady-state" curve shown in Fig. 7. In the plot, the *y*-axis has been labelled "Relative activity–PO_x effect" in order to underline that the curve represents the deactivation explicitly due to the polyphosphoric acids poisoning. As it can be seen, this mechanism caused a deactivation rate of 0.2% day^{-1} until about 750 h of exposure, after which the rate became nil, indicating a steady-state between P-deposition and loss by hydrolysis. At the end of the exposure, the percentage of total deactivation that could be associated to poisoning by PO_x was estimated equal to about 6–7%.

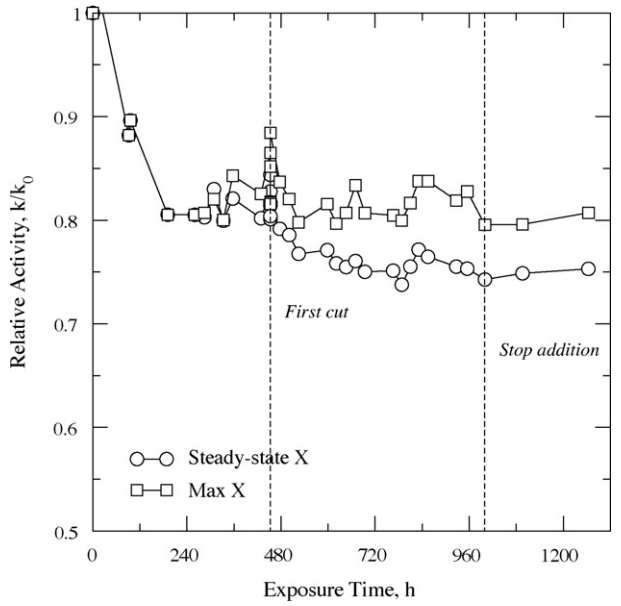

Fig. 7. Relative activity as a function of exposure time. The activity measurements were made at 350 °C. Gas dry composition: NO = 500 ppmv, NH_3 = 600 ppmv, O_2 = 10 vol.%, CO_2 = 6 vol.%, H_2O = 10 vol.%. Flow: 40 Nm^3/h. The "Max X" data set represents the maximum NO conversion obtained during each single activity measurement, whereas the "Steady-state X" data set represents the final NO conversion obtained during the same measurements. The samples ADD1T and ADD1B were taken at the time indicated by "First cut".

Apart from the quantification of the so-called "PO_x effect", another important conclusion can be made from Fig. 7. Since the appearance of the NO conversion transient, the "Max X" relative activity has constantly remained around 81% throughout the whole exposure. In fact, 19% of the original activity was lost after the first 191 h of exposure, where no NO transient was measured. This result indicates that the components causing the fast drop of activity at the beginning of the exposure did not cause any further deactivation during the rest of exposure.

3.3.2. NH_3 chemisorption tests

The NH_3 chemisorption tests made before the first cut off of the top and bottom 5 cm are reported in Table 3, together with the observed steady-state relative activity for comparison, in order to understand the mechanism of deactivation that caused the steep initial decrease in relative activity. According to the NH_3 chemisorption tests, the 19% decrease of activity measured after 260 h of exposure was accompanied by a loss of only 16% in the total chemisorbed NH_3. A higher decrease in the relative amount of chemisorbed NH_3 compared to the decrease in relative activity would have been measured, if poisoning by K and/or Ca was the main responsible for the measured deactivation. This is because the monolith is operating under both external and internal mass

Table 3
Relative chemisorbed NH_3 and relative activity as a function of exposure time.

Time (h)	NH_3 (mol/kg)	NH_3/NH_{30}	k_{ss}/k_0
0	0.033	1.00	1.00
260	0.028	0.84	0.81
333	0.028	0.84	0.80
357	0.029	0.86	0.82

transfer limitations, which are partially masking the effect of chemical deactivation on the intrinsic rate of reaction. Assuming (i) a square root dependency between intrinsic rate of reaction and the observed rate of reaction, valid for mass-transfer-limited reactions; and (ii) a linear relation between the chemisorbed NH_3 and the intrinsic activity, it can be calculated that poisoning only accounted for 8% of the lost activity. The remaining 11% was instead due to physical deactivation by pore blocking and surface masking.

After the first cut of material, a relative increase of chemisorbed NH_3 was measured. For instance, the element increased its capacity in chemisorbing NH_3 of about 39% in the last 600 h of exposure. This increase in chemisorbed NH_3 was found in our previous investigation to be related to the presence of polyphosphoric acids in the catalyst [15], which form P-sites where NH_3 can chemisorb. However, these sites are either *less active*, in agreement with Kamata et al. [13], or inactive, thus simply constituting an NH_3-storage on the surface.

Similarly to our previous investigation [15], higher NO conversions could be obtained by increasing the NH_3 partial pressure in the flue gas, as shown in Fig. 9, where a standard activity measurement made after 1096 h of total exposure (i.e. after 1000 h exposure to the doped flue gas and 96 h exposure to a clean flue gas) followed by a test with the double amount of NH_3 introduced (i.e. 1200 ppmv) is reported. This additional activity at higher NH_3 partial pressures is related to changes in the NH_3 adsorption constant of the catalyst surface. It can then be argued that, due to the increased number of sites for the NH_3 chemisorption, the coverage of NH_3 appearing in Eq. (1.1) has become less than 1 at the typical condition of our activity measurements.

3.4. Activity measurements in the laboratory and Hg-porosimetry tests

Activity tests on powder samples have been carried out in the laboratory in order to more clearly identify the extent of deactivation measured on the monolith due to poisoning. Fig. 10 shows an Arrhenius plot of the activities of the fresh and spent

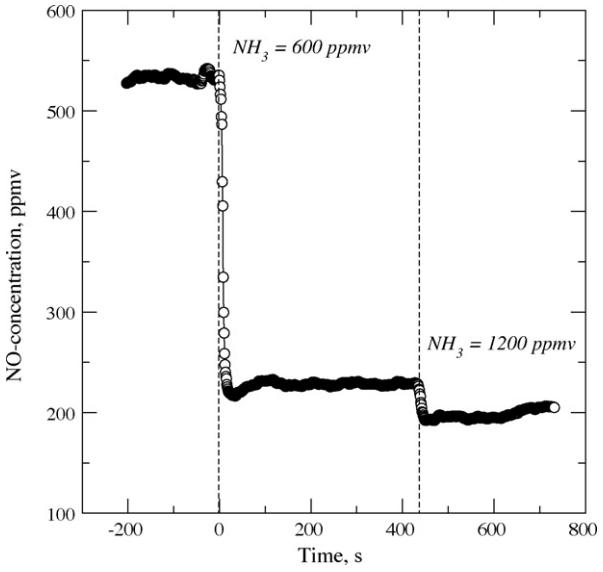

Fig. 9. Activity measurement on spent catalyst exposed for 1000 h to the doped flue gas and 96 additional hours to a clean flue gas. $T = 350\ ^\circ C$. Gas dry composition: NO = 500 ppmv, NH_3 = 600–1200 ppmv, O_2 = 10 vol.%, CO_2 = 6 vol.%, H_2O = 10 vol.%. Flow: 40 Nm^3/h.

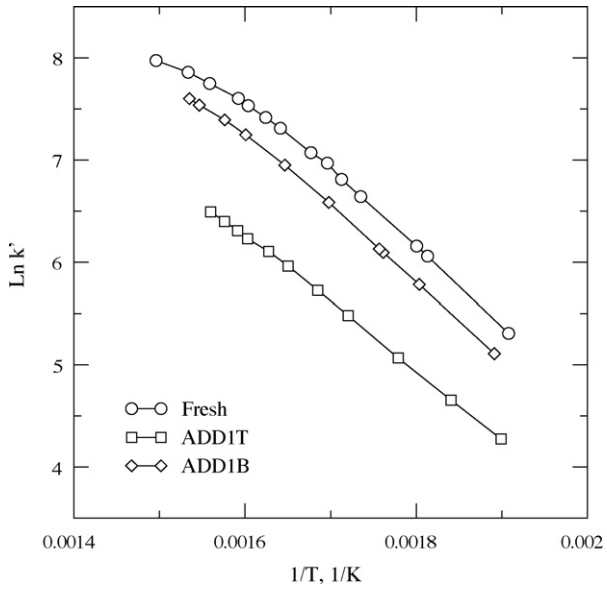

Fig. 10. Activity test on powder samples. Catalyst mass, $W = 0.07$ g. Total flow $F = 2.8$ Nlitre/min. Gas composition: NO = 500 ppmv, NH_3 = 600 ppmv, O_2 = 5%, H_2O = 1.4% in N_2.

catalyst samples exposed for 453 h (i.e. ADD1T and ADD1B). The plot only reports the results in the temperature range 250–400 °C. In this range of temperatures, at the chosen experimental conditions, no external mass transfer limitations are present. Due to their high activities, both the fresh and ADD1B samples are subjected to some internal mass transfer limitations, as shown by the bending of the straight line at the higher temperatures in the Arrhenius plot. In particular, diffusion free conditions for the ADD1T and ADD1B samples are obtained at 326 and 337 °C, respectively. The samples ADD1T and ADD1B had a relative activity of 27% and 75%, respectively. These values were constant in the whole temperature range as indicated by the same activation energy calculated from the Arrhenius plot (i.e. 63 kJ/mol).

Physical deactivation by formation of the external layer has been pointed out by the Hg-porosimetry analysis. Fig. 11 shows the pore size distribution for the fresh sample and ADD2B, which, as shown by the SEM pictures, presented a fouling layer on its external surface. As it can be seen in the figure, the ADD2B sample did not present any pores in the range 0.3–8 μm. However the total intrusion volume did not differ between the two samples. This fact indicates that the outer surface of the ADD2B sample only presents pores smaller than 0.3 μm due to the formation of the fouling layer causing pore mouth closure.

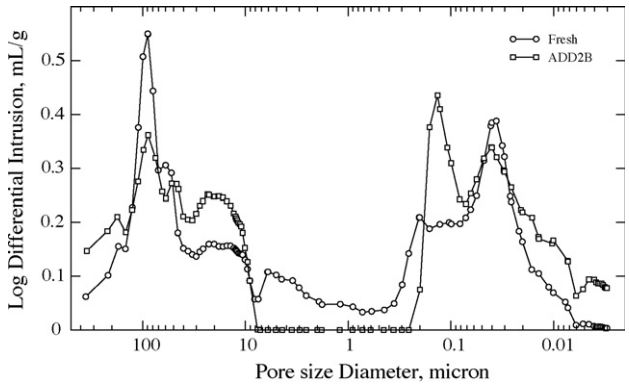

Fig. 11. Pore size distribution measured by Hg-porosimetry.

4. Discussion

4.1. Polyphosphoric acids formation

Based on the results obtained in a previous investigation about deactivation by polyphosphoric acids [15] and the results just described in this work (i.e. aerosol formation by homogeneous nucleation, NO conversion transient, increased amount of chemisorbed NH_3, activity dependency on NH_3 partial pressures), there is no doubt about their formation during the exposure to the additive mixture in this work. The reasons for their formation during this particular test can be various, but they would all require the formation of gaseous H_3PO_4 and its exposure to temperatures higher than 600–700 °C. It is believed that some of the compounds which were formed during evaporation of the water from the atomized droplets went through decomposition at increasing temperatures and released some H_3PO_4 in the gas phase. This latter might also have been formed directly during the spraying process. At the end of the polyphosphoric acid investigation [15], it was not clear whether the formation would have been possible in a system including other different elements, or whether the formation was the result of the simplified flue gas composition used in those tests. The results obtained in this investigation have shown that the formation of polyphosphoric acids was possible in our system at the given P/K and P/Ca ratios. Depending on their concentration, polyphosphoric acids may constitute a high risk for a fast deactivation of the vanadia-based SCR catalysts, since for concentrations corresponding to 100 ppmv H_3PO_4, their deposition might already be too fast compared to the rate of hydrolysis at SCR reaction conditions.

4.2. Particle deposition and penetration

The volume-based particle size distributions measured by the SMPS and the SEM pictures of the deposits have shown the presence of two distinct classes of particles. The first one with a volume-based mean diameter equal to 12 nm, and the second one with a volume-based mean diameter equal to 300 nm. Due to both a higher number concentration and a higher diffusion coefficient, the first class of particles is depositing faster than the other. By associating these particles to the polyphosphoric acids, which are liquid at the SCR temperatures, it can be assumed that the P found inside the catalyst walls is mainly due to their depositions and penetration due to capillary forces. On the other hand, the complete absence of Ca and K inside the walls is an indication that: (i) these elements are present in the bigger particles (i.e. $d_p > 0.1$ μm) which have lower deposition rates and practically no penetration ability; (ii) they are tightly bound to the particles themselves. This latter indication is particularly interesting since it further supports the mechanism of deactivation by K proposed in previous works [3,11]. It is now clear that the K present in the particles which are deposited on the outer surface of the catalyst needs to be released from the particles on atomic scale by interactions with the catalyst surface. It is only afterwards that K can diffuse inside the walls by surface concentration gradients. Particle diffusion is not likely to happen since the same mechanism would have also been active in this investigation, due to the similar particle sizes involved in the tests. K and Ca are instead accumulating on the outer surface. Due to the higher concentration of P found on the formed fouling layer, it is likely that the K–Ca–(P) crystals are glued together by deposited polyphosphoric acids forming the molten-looking layer. This fact would then indicate that the polyphosphoric acids can be regarded as fouling promoters. From the present data it is not possible to know whether this outer layer would have continued growing or whether its thickness had reached a steady value. From the cracks found during the SEM analysis, it appears that some of it has fallen apart, but this could have happened during the cooling of the monolith and may not happen during normal operation.

Regarding the S-content, the SO_2 levels measured in the flue gas were approximately the same as those calculated by assuming the entire S added by the solution to be completely converted to SO_2. Therefore it is believed that the additional S found on the outer surface of the catalyst is due to sulphation reactions between the deposits and the gaseous SO_2. Moreover, since no additional S has been found inside the catalyst wall where only P had accumulated, it is assumed that the sulphation reaction preferentially takes place with K and Ca giving K_2SO_4 and $CaSO_4$, respectively.

4.3. Deactivation mechanism

Based on the results presented, it can be concluded that the deactivation measured during this investigation followed different mechanisms, each of them acting in different periods of time. During the first 200 h of exposure, the steep decrease in observed deactivation (i.e. 2.4% day^{-1}) was mainly due to physical deactivation surface fouling and blocking of the macro-cracks caused by particle deposition on the catalyst outer surface, with subsequent direct and indirect blocking of the active sites. Due to the pore blocking, the diffusion of both reactants and products is slowed down and, even though the inner layers of the wall are still very active since not attacked by the poison, they are less accessible. This mechanism of deactivation, however, is not expected to cause any further deactivation in the long term provided that the formed deposit layer will (i) keep some porosity, and (ii) not increase its thickness.

For exposure time >300 h, the observed deactivation was instead due to poisoning by polyphosphoric acids and initially proceeded at 0.2% day^{-1} and reached a steady-state level after about 750 h of exposure. Based on both the size and number concentration of the particles which have been assigned to the polyphosphoric acids (i.e. the peak around 9 nm) and the aerosols measurements made at different H_3PO_4 concentrations in a previous investigation [15], it can be estimated that these were counting for about 3–4 ppmv P during the test reported in this work, i.e. half of the total P injected in the flue gas. At these low concentrations, P-accumulation in the catalyst walls is limited by the hydrolysis of the polyphosphoric acids at the SCR temperature by the gas moisture [15]. Therefore, it is believed that the relative activity levelled off due to a steady-state PO_x-level in the catalyst wall obtained due to simultaneous deposition and hydrolysis.

Based on these considerations, it is not expected that further deactivation due to the just discussed mechanisms would have been measured if the exposure was continued.

5. Conclusion

Simultaneous addition of KCl, H_3PO_4, $Ca(OH)_2$ and H_2SO_4 in a hot flue gas has been carried out for 1000 h and a commercial SCR catalyst has been exposed to the resulting flue gas while the activity was followed as a function of exposure time. The test has been used to estimate the effects of the potential products of the K-getter additives during biomass combustion. In the test carried out, the P/K and P/Ca molar ratios have been fixed to values of 2 and 0.8, respectively, suggested in the literature.

Either K or Ca did penetrate the catalyst walls but only accumulated on the external catalyst surface. Poisoning by K and

Ca was therefore limited to the most outer wall layers. It has been estimated that 8% of initial relative activity (i.e. about 1/3 of the overall deactivation measured at the end of the test) was lost due to this mechanism, whereas 11% was lost due to physical deactivation by fouling and pore blocking.

At the chosen experimental conditions, formation of polyphosphoric acids has been favoured and about half of the total P has been estimated to be present in these compounds, which formed aerosols with volume-based mean diameter equal to 12 nm. The known deactivating effects of the polyphosphoric acids (i.e. NO transient, activity dependency on NH_3 partial pressures) have been identified: after the initial loss of activity, they controlled the overall deactivation rate, which was about 0.2% day^{-1}. However, due to their relatively low concentration and the simultaneous occurrence of hydrolysis at the SCR reaction condition, the catalyst activity reached a steady-state after about 750 h of exposure. No additional deactivation was then measured in the following 250 h of addition.

Based on the results obtained in this work, it can be concluded that binding K into P–K–Ca compounds is an effective way of reducing the deactivation rates normally experienced during biomass combustion. Reactions between K and the V active sites are in fact prevented, and so is the penetration of K in the catalyst walls by surface diffusion. However, in real applications, the formation of polyphosphoric acids needs to be controlled, since this may counterbalance the just mentioned positive effects by promoting fouling and by poisoning the active sites. In particular, regarding the poisoning, PO_x levels in the range 1–10 ppmv may still be acceptable since their accumulation will be limited by their simultaneous hydrolysis, and a steady-state level in the catalyst wall will be reached. This situation could however be different in the presence of higher K-concentrations in the flue gas. If the fraction of P forming the PO_x is mainly controlled by the P/K and P/Ca ratios, at higher K-contents the amount of formed PO_x could be higher and thereby lead to faster deactivation rates. More tests at different P/K and P/Ca ratios would be necessary to understand the formation of PO_x, and suggest the conditions to limit it.

Acknowledgments

This work is part of the CHEC (Combustion and Harmful Emission Control) Research Center funded a.o. by the Technical University of Denmark, the Danish Technical Research Council, the European Union, the Nordic Energy Research, Dong Energy A/S, Vattenfall A.B., F L Smidth A/S, and Public Service Obligation funds from Energinet.dk and the Danish Energy Research program. In particular, this work is supported by the PSO project "Deactivation of SCR Catalysts by Additives" (PSO Elkraft FU-4205). Supply of the catalyst samples by Haldor Topsøe A/S is gratefully acknowledged.

References

[1] F. Castellino, A.D. Jensen, J.E. Johnsson, Applied Catalysis B: Environmental 86 (2009) 166–175.
[2] P.A. Jensen, L.H. Sørensen, G. Hu, J.K. Holm, F. Frandsen, U.B. Henriksen. Technical University of Denmark (2005) KT-Report No. 0504.
[3] Y. Zheng, A.D. Jensen, J.E. Johnsson, Applied Catalysis B: Environmental 60 (2005) 261–272.
[4] Å. Kling, C. Andersson, Å. Myringer, D. Eskilsson, S.G. Järås, Applied Catalysis B: Environmental 69 (2007) 240–251.
[5] J.P. Chen, M.A. Buzanowski, R.T. Yang, Journal of the Air and Waste Management Association 40 (1990) 1403–1409.
[6] J.P. Chen, R.T. Yang, Journal of Catalysis 125 (1990) 411–420.
[7] L. Lietti, P. Forzatti, G. Ramis, G. Busca, F. Bregani, Applied Catalysis B: Environmental 3 (1993) 13–35.
[8] H. Kamata, K. Takashi, C.U.I. Odenbrand, Journal of Molecular Catalysis A: Chemical 139 (1999) 189–198.
[9] R. Khodayari, C. Andersson, C.U.I. Odenbrand, L.H. Andersson, Proceeding of the Fifth European Conference on Industrial Furnace and Boilers, Vol. II, Espinho, Porto, Portugal, 11–14 April, 2000.
[10] Y. Zheng, A.D. Jensen, J.E. Johnsson, Industrial and Engineering Chemistry Research 43 (2004) 941–947.
[11] Y. Zheng, A.D. Jensen, J.E. Johnsson, Applied Catalysis B: Environmental 83 (2008) 186–194.
[12] J. Blanco, P. Avila, C. Barthelemy, A. Bahamonde, J.A. Odriozola, J.F. Garcia de la Banda, H. Heinemann, Applied Catalysis 55 (1989) 151–164.
[13] H. Kamata, K. Takahashi, C.U.I. Odenbrand, Catalysis Letters 53 (1998) 65–71.
[14] J. Beck, J. Brandenstein, S. Unterberger, K.R.G. Hein, Applied Catalysis B: Environmental 49 (2004) 15–25.
[15] F. Castellino, S.B. Rasmussen, A.D. Jensen, J.E. Johnsson, R. Fehrmann, Applied Catalysis B: Environmental 83 (2008) 110–122.
[16] N.-Y. Topsøe, T. Slabiak, B.S. Clausen, T.Z. Srnak, J.A. Dumesic, Journal of Catalysis 134 (1992) 742–746.